Monodomain strained ferroelectric $PbTiO_3$ thin films: Phase transition and critical thickness study

Sriram Venkatesan,[1] Ard Vlooswijk,[2] Bart J. Kooi,[1,*] Alessio Morelli,[1] George Palasantzas,[1] Jeff T. M. De Hosson,[1] and Beatriz Noheda[2]

[1]*Department of Applied Physics, Zernike Institute for Advanced Materials, University of Groningen, Nijenborgh 49747 AG Groningen, The Netherlands*

[2]*Department of Chemical Physics, Zernike Institute for Advanced Materials, University of Groningen, Nijenborgh 49747 AG Groningen, The Netherlands*

(Received 10 July 2008; published 18 September 2008)

This work demonstrates that instead of paraelectric $PbTiO_3$, completely *c*-oriented ferroelectric $PbTiO_3$ thin films were directly grown on (001)-$SrTiO_3$ substrates by pulsed-laser deposition with thickness up to 340 nm at a temperature well above the Curie temperature of bulk $PbTiO_3$. The influence of laser-pulse frequency, substrate-surface termination on growth, and functional properties were studied using x-ray diffraction, transmission electron microscopy, and piezoresponse force microscopy. At low growth rates (frequency <5 Hz) the films were always monodomain. However, at higher growth rates (frequency >8 Hz) *a* domains were formed for film thickness above 20–100 nm. Due to coherency strains the Curie temperature (T_c) of the monodomain films was increased approximately by 350 °C with respect to the T_c of bulk $PbTiO_3$ even for 280-nm-thick films. Nonetheless, up to now this type of growth mode has been considered unlikely to occur since the Matthews-Blakeslee (MB) model already predicts strain relaxation for films having a thickness of only ~10 nm. However, the present work disputes the applicability of the MB model. It clarifies the physical reasons for the large increase in T_c for thick films, and it is shown that the experimental results are in good agreement with the predictions based on the monodomain model of Pertsev *et al.* [Phys. Rev. Lett. **80**, 1988 (1998)].

DOI: 10.1103/PhysRevB.78.104112 PACS number(s): 77.80.Bh, 77.84.Dy, 68.37.−d, 61.05.cp

I. INTRODUCTION

Ferroelectric thin films are subject of current interest because of important applications, e.g., in electromechanical transducers, accelerometers, micropositioners, etc., and their promising use for nonvolatile memories. Although miniaturization and nanoscaling have led to effects that modify the ferroelectric behavior, the latter still requires improved fundamental understanding in the reduced dimensions.[1] In particular for epitaxial ferroelectrics, the misfit strain largely affects the behavior and properties of the thin films.[2–5] Several theoretical models were developed, predicting the effect of substrate constraints on domain structures in ferroelectric films.[6–11] Clearly, in order to apply these models a detailed understanding of the precise boundary conditions is required. This is a subject area that is still shrouded with considerable confusion. For instance, the model of Koukhar *et al.*[9] for dense domain structures predicts an equilibrium volume fraction of *c* domains, i.e., having the *c* axis perpendicular to the surface, of 80% in $PbTiO_3$ (PTO) films grown on (001)-$SrTiO_3$ (STO) substrates. However, the models of Pertsev *et al.*[7] and Alpay and Roytburd[8] for the same strain predict the formation of completely *c*-oriented films.

In general, relatively thick PTO films (i.e., >50 nm) grown at a temperature above the Curie temperature (T_c) of bulk PTO are considered to have a cubic paraelectric phase.[2,3,6,8–10] Domain structures arise when this phase is cooled through T_c. In such a case the models of Koukhar *et al.*[9] and Li *et al.*[10] can be applied. Ultra-thin-films (i.e., <10 nm) are generally considered to be coherently strained by the substrate and therefore the "single-domain" model of Pertsev *et al.*[7] can be applied when the additional effects of, e.g., depolarization fields resulting in 180° domains are included.[11–13] (Note that we neglect the potential presence of 180° domains when we adopt the term single-domain or monodomain for our relatively thick PTO films.) A distinction between thin and thick films can be made because the former are considered to coherently match the substrate, while the latter are beyond the critical thickness where strain relaxation by misfit dislocations takes place. Experimental validation or theoretical calculation of the critical thickness thus becomes important to make the proper distinction.[14]

For ferroelectric films with the seminal work by Speck and Pompe,[6] the Matthews-Blakeslee (MB) model[15] has become the most popular approach for calculating the critical thickness. Also in the related use of the effective substrate lattice parameter (b^*), accounting for the reduced mismatch a film experiences from the substrate due to introduction of a misfit dislocation density, the MB model became influential.[6–9,11,14] This model predicts for PTO on (001)-STO a relatively small critical thickness of the order of only 10 nm.[6,14] However, it has been shown that the MB model works well for metals but strongly underestimates the critical thickness in semiconductor films, particularly at relatively low strains.[16–19] Arguments that explain the too low values of the MB critical thickness for semiconductor films apply also to ferroelectric films. In particular in the case of high quality films and substrates where initial (threading) dislocations are absent, the actual nucleation of and (Peierls) friction force on the dislocations prevent the MB model to be directly applicable.[16–19] Therefore it is possible to grow coherently strained films on high quality substrates that are more than

ten times thicker than that predicted by the MB model.[16,17] Subsequently, the film thickness where, e.g., either the model of Pertsev *et al.* or the one of Koukhar *et al.* applies can shift dramatically.

Ferroelectric films can exploit a different mechanism to prevent or at least reduce strain relaxation by misfit dislocations if the films are grown at a temperature above the T_c of the bulk ferroelectric material. The film can grow directly in the unstable ferroelectric state (from a bulk point of view) instead of the stable paraelectric state and use the spontaneous strains associated with the paraelectric to ferroelectric phase transition to reduce the mismatch with the substrate. This reduced mismatch will increase the critical thickness and reduce the misfit dislocation density beyond the critical thickness.

Although coherent ferroelectric films, typically with a thickness of 100–150 nm and thus beyond the expected strain-relaxation thickness, have been previously reported,[20–22] an adequate explanation for this effect is still absent and will be provided by the present work. Moreover, it will be shown for the first time that completely *c*-oriented strained PTO films as thick as 280–340 nm can be grown in "equilibrium" coherently on (001)-STO, i.e., without any *a*-domain formation after cooling to room temperature. The large increase in T_c we observed for such thick films, as induced by the coherency strains, has not been reported before. The present work will explain why our experimental results show good agreement with the monodomain model of Pertsev *et al.*,[7] whereas previously the polydomain model of Koukhar *et al.*[9] was adopted[2,3] for PTO films (with thickness above 10 nm) on (001)-STO substrates.

II. EXPERIMENTAL PROCEDURE

Single-crystalline *c*-oriented $PbTiO_3$ films ranging in thickness from 22 to 340 nm were grown by us on (001)-STO substrates at 570 °C using pulsed-laser deposition. The influences of the growth parameters, substrate-surface terminations, and functional properties of the synthesized films have been analyzed. For the analysis we used x-ray diffraction (XRD), also as a function of temperature, transmission electron microscopy (TEM), atomic force microscopy (AFM), and piezoresponse force microscopy (PFM).

Low miscut (<0.2°) cubic (001)-$SrTiO_3$ substrates (lattice parameter 3.905 Å at room temperature), matching with bulk single-crystal $PbTiO_3$ lattice parameters ($a=b=3.902$ Å and $c=4.156$ Å at room temperature[23]), were used. The substrate-surface treatment followed the procedure outlined by Koster *et al.*[24] The PTO thin films were grown at 570 °C using reflection high-energy electron diffraction assisted pulsed-laser deposition (KrF excimer laser of $\lambda=248$ nm). A laser spot size of 2.5 mm^2 with an energy density of 2 J/cm^2 at an oxygen background pressure of 0.13 mbar was used, and the substrate-target distance was kept between 48 and 51 mm. All grown films were annealed in 0.5 bar of O_2 and cooled at a rate of 5 °C/min except for two samples that on purpose were cooled rapidly. Films were grown with laser-pulse frequencies varying from 0.5 to 15 Hz. The growth per laser pulse was 0.4 ± 0.1 Å for the used frequency range, i.e., leading to growth rates in between 0.2 and 6 Å/s. 40-nm-thick $SrRuO_3$ bottom electrodes were deposited at 600 °C with a 2 Hz laser frequency for the PFM measurements.

The surface morphology of the chemically treated substrates prior to deposition was studied using AFM. A Dimension 3100 SPM was used for local PFM measurements, which were performed with conductive Si cantilevers with a spring constant of 40 N/m and a modulation voltage (having a frequency of 5 kHz) 3 V *peak to peak* (V_{pp}) applied to the sample. Local polarization reversal of the as-deposited PTO film was obtained by applying a dc voltage of 4 V to the tip at a scanning speed of 2 μm/s.

X-ray diffraction experiments have been performed on our PanAlytical X'Pert four axes diffractometer with Anton Paar heating stage. This setup is equipped with a Cu x-ray generator tube supplying x-rays with a $\lambda=1.540\,598$ Å (Cu $K\alpha$). In Bragg-Brentano configuration, both x-ray reflectivity and out-of-plane diffraction measurements at temperatures up to 900 °C can be performed, providing information on film thicknesses and lattice parameters. The coherency (incoherency) of the thin films and domain formation have been studied by recording reciprocal space maps, mainly in the (00L) and (H0L) planes.

Finally, the TEM observations were performed with a JEOL 2010F transmission electron microscope operating at an accelerating voltage of 200 kV. The cross-section samples were prepared by the conventional method involving cutting, grinding, polishing, dimpling, and ion milling. A precision ion polishing system (Gatan model 691) with 4kV Ar^+ beams having incident angle of 8° on both sides was used.

III. RESULTS

The choice of single-crystal substrates and their surface treatment are crucial for the quality of the film because the substrate-film interface plays a major role in the epitaxial growth, strain relaxation, and formation of misfit dislocations. AFM images of the treated substrates confirmed the presence of large atomically flat terraces separated by steps with only unit-cell height of 0.4 nm indicating perfect TiO_2 termination[24] [Figs. 1(a) and 1(b)]. Sometimes the same treatment resulted in a mixed SrO/TiO_2 termination (including half unit-cell height steps). Substrates showing single termination have an rms roughness of approximately 1.3 Å, and substrates having a mixed termination show a slightly higher roughness. Figure 1(c) shows an AFM image after deposition of a 280-nm-thick PTO film on a perfect TiO_2 terminated substrate. The PTO film exhibits a uniform flat surface with an rms roughness of 10 Å.

The PTO films of various thicknesses were grown using different laser-pulse frequencies, keeping other growth parameters constant. The growth per laser pulse was 0.4 ± 0.1 Å for the frequency range used. Figure 2 shows simultaneously the laser-pulse frequency and growth rate versus the film thickness, indicating also the regime of presence or absence of *a* domains in the films as observed by XRD and/or TEM. The results can be summarized as follows: In films grown at low laser-pulse frequencies

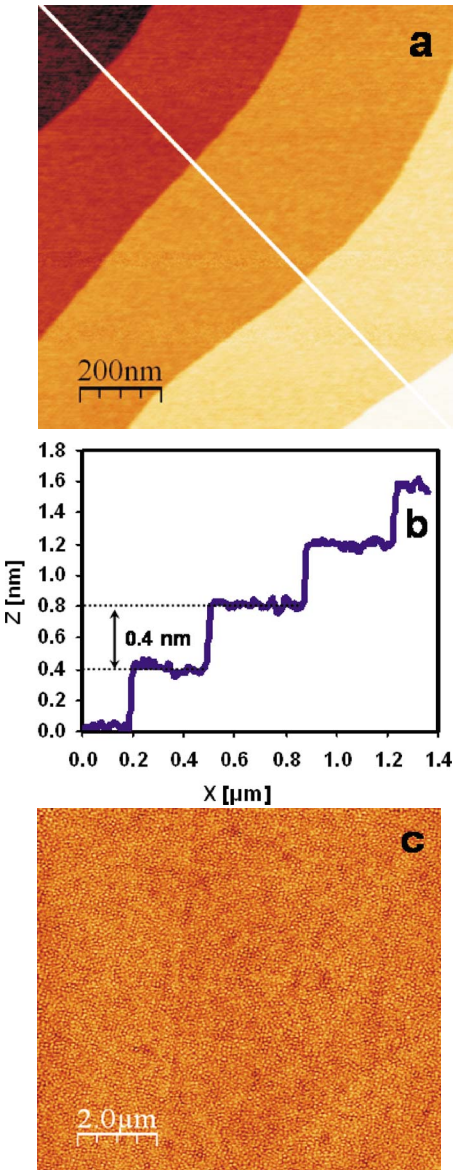

FIG. 1. (Color online) AFM micrograph showing (a) the surface of a chemically treated $SrTiO_3$ substrate, before deposition, with atomically flat terraces separated by steps of unit-cell height, (b) line profile of the treated substrate showing the step height of 0.4 nm, and (c) the surface of a 280-nm-thick $PbTiO_3$ film after deposition on a (nearly perfect) TiO_2 terminated substrate.

($\leq$5 Hz), *a* domains did not develop up to large thickness (at least 280–340 nm) even for the substrates with mixed SrO/TiO_2 terminations. In this frequency regime the cooling rate did not affect the completely *c*-oriented films. Two of the films grown at 1 Hz to thickness of 170 and 340 nm were cooled more rapidly by turning off the substrate heater holder but still *a* domains were not introduced by the much faster cooling. From our earlier experiments we have optimized the growth conditions for PTO films. Indeed, one film was grown at a higher O_2 background pressure but no formation of *a* domains was detected.

On the other hand, at high laser-pulse frequencies ($\geq$8 Hz) *a* domains develop above a critical thickness, typically $\sim$20–100 nm, even for nearly perfect TiO_2 terminated

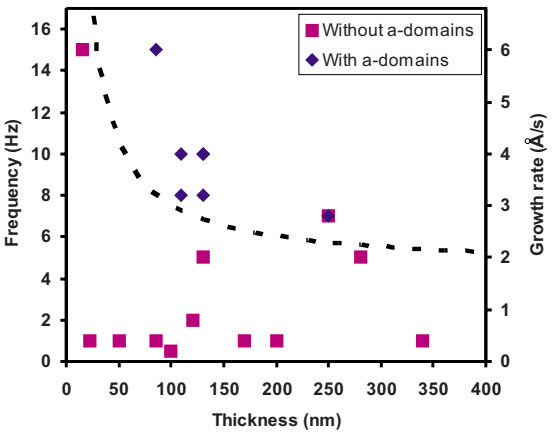

FIG. 2. (Color online) Graph of laser-pulse frequency (growth rate) versus $PbTiO_3$ film thickness showing the presence or absence of *a* domains in the films as observed using XRD and/or TEM. The dashed line is a guide to the eye to distinguish the regions with and without *a* domains.

substrates. In these cases secondary phases were generally detected (XRD/TEM), which are expected to act as nucleation sites for *a*-domain formation during growth or more likely during cooling. At intermediate laser-pulse frequencies (between 5–8 Hz) *a* domain formation can be avoided up to large thickness (at least up to 250 nm) when the substrate has perfect TiO_2 termination; with less perfect substrate surfaces (i.e., mixed termination) *a* domains did occur in 250-nm-thick films.

XRD was performed and reciprocal space maps were collected to investigate the crystallinity and to verify the domain structure in all samples. An example of a $\theta-2\theta$ x-ray diffraction pattern of a 130-nm PTO film grown with 8-Hz laser-pulse frequency on a 30-nm $SrRuO_3$ bottom electrode covering the STO substrate is shown in Fig. 3(a). Only a single phase, i.e., the tetragonal perovskite PTO is observed in the films and no secondary phases were detected for growth frequencies $\leq$8 Hz. The reciprocal space map around the (002) Bragg reflection of a 280-nm-thick PTO film grown with 5 Hz [Fig. 3(b)] shows that the film is epitaxial and *c* oriented, and confirms the absence of *a* domains.

TEM was employed to view structural details at the substrate-film interface and presence of any defects such as threading and misfit dislocations, and also to confirm the absence of 90° domains locally. Figure 4(a) shows the cross-section bright-field TEM image of a 280-nm PTO film on STO, which again confirms that the film is monodomain single-crystal at this more local scale. High-resolution TEM images of the substrate-film interface always indicates that misfit dislocations are absent, confirming the coherent interface matching [Fig. 4(b)].

Temperature-dependent XRD was performed to study the transition of PTO from tetragonal ferroelectric to cubic paraelectric with the accompanying changes in lattice parameters during heating and cooling between room temperature and 700 or 800 °C.[25] Figure 5 shows the *c*-axis value of PTO plotted versus temperature for completely *c*-axis oriented films having a thickness of 130 and 280 nm, and the measured STO lattice parameter. The solid lines drawn in

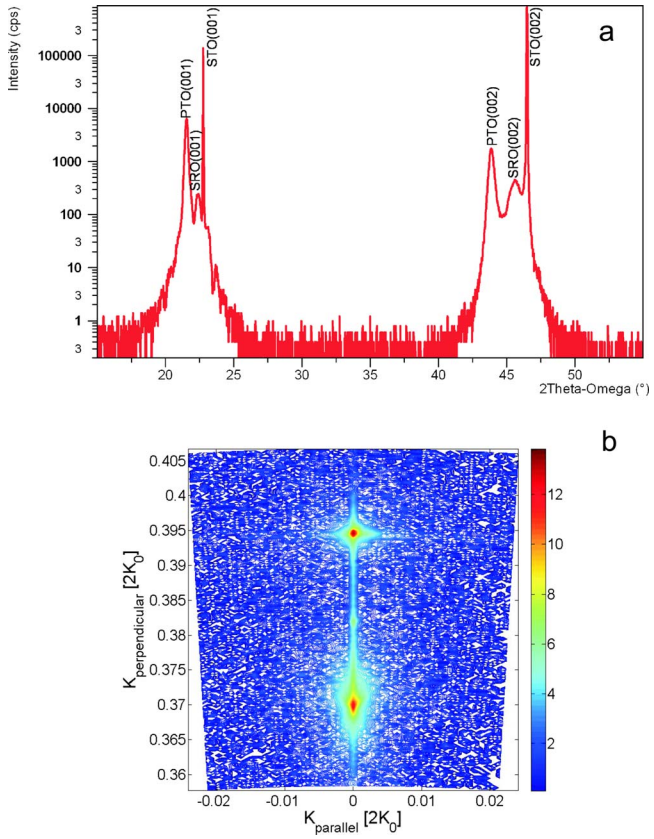

FIG. 3. (Color online) X-ray diffraction patterns: (a) $\theta-2\theta$ scan of a 130-nm-thick $PbTiO_3$ film on a $SrRuO_3$ bottom electrode on a $SrTiO_3$ substrate indicates the absence of secondary phases in the $PbTiO_3$ and (b) reciprocal space map around the (002) reflection of a 280-nm-thick $PbTiO_3$ film on $SrTiO_3$ (in units of $2K_0=4\pi/\lambda=4\pi/1.540\ 598$ Å) confirms the absence of *a* domains in the completely *c*-oriented $PbTiO_3$ film.

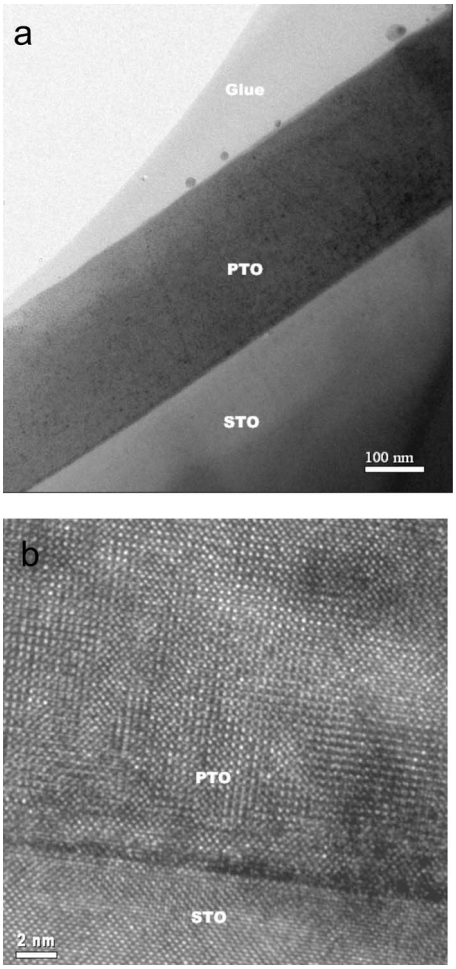

FIG. 4. TEM images of a 280-nm $PbTiO_3$ film on $SrTiO_3$; (a) bright-field image showing the absence of *a*-domains and (b) high-resolution image showing a substrate-film interface free of misfit dislocation.

Fig. 5 are theoretical results that will be explained below.

The experimental results demonstrate that the T_c of both films is much higher than that of bulk PTO ($T_c^{\text{bulk}}=492$ °C).[26] For the 280-nm film T_c is between 650 and 675 °C, and for the 130-nm-thick film the T_c is higher than 700 °C. Apart from this difference in T_c, the thicker film has a higher *c*-axis value at low temperatures compared to the 130-nm film. At room temperature the *c*-axis value for the 280-nm-thick film is slightly higher than that reported for bulk PTO,[23,26] whereas for the 130-nm film it is slightly lower. The variations in *c*-lattice parameters may be related to the presence of oxygen (and lead) vacancies, which can possibly also affect relaxations. Nevertheless, Fig. 5 proves that such types of relaxation are secondary effects because both films still show a large increase in T_c with respect to bulk PTO.

Finally, in order to prove the ferroelectric character of our films, we performed PFM measurements. An example of retention loss measurements, performed on a 130-nm-thick PTO film grown at 0.5 Hz frequency, is shown in Fig. 6. Initially, the as-deposited film exhibited upward polarization. Then, PFM was used to write an area of $1\times1\ \mu m^2$ in the opposite, i.e., downward polarization. Plotting the fraction of area that loses the down polarization (i.e., reverses back to the up polarization) as a function of time, we obtain an exponential growth, which can be fitted by a stretched exponential ($A\{1-\exp[-(t/k)^d]\}$) indicating a dispersive transport or random-walk type process.[27] The effective inversion time *k* from the fit is $k=376$ h, comparable with retention times observed in heteroepitaxial PTO (Ref. 28) and in polycrystalline PZT films,[27] indicating therefore sufficiently long retention in our films.

IV. DISCUSSION

The present results show that using low laser-pulse frequencies, i.e., low growth rates, completely *c*-oriented PTO films can be grown at 570 °C on (001)-STO up to a thickness of 340 nm. Only when increasing the growth rate, i.e., moving away from thermodynamic equilibrium, *a* domains developed in the films.

The deposition temperature of 570 °C is above 492 °C, the T_c of bulk PTO. As bulk, tetragonal ferroelectric PTO is unstable at the deposition temperature with respect to the cubic paraelectric phase. However, incorporating strain energy due to the lattice mismatch of these two PTO phases

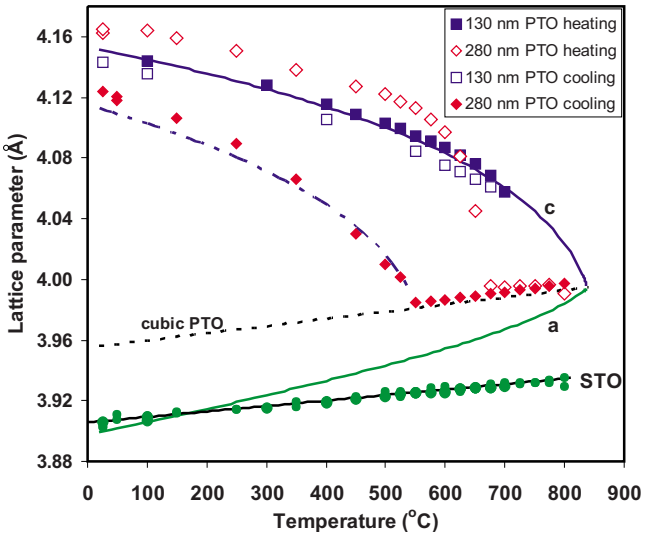

FIG. 5. (Color online) Results of temperature-dependent XRD measurements showing the *c*-axis lattice parameters of 130- and 280-nm-thick monodomain PTO films as a function of temperature during heating and cooling. Also the measured lattice parameters of the $SrTiO_3$ substrate are given. Lines represent theoretical results as explained in the main text. The dashed line holds for strain-free cubic PTO and is important to calculate the misfit strain that is the input parameter of the model of Pertsev *et al.* (Ref. 7). The solid lines are predictions of the model for the PTO without using any adjustable parameter. The agreement with the 130-nm-thick film (during heating) is excellent. The dashed-dotted line is a prediction of the model when assuming that 80% of the strain is relaxed. Then, excellent agreement is achieved with the results obtained during cooling of the 280-nm-thick PTO film.

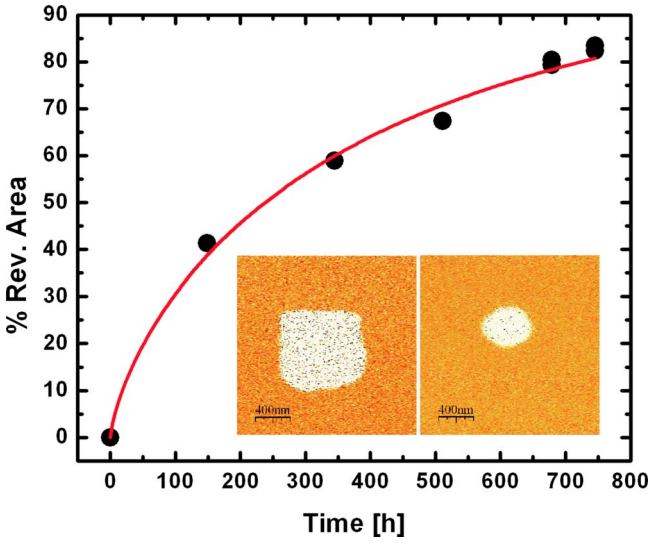

FIG. 6. (Color online) Retention loss data when fitted using the function $A\{1-\exp[-(t/k)^d]\}$ gives the following fit parameters: $d=0.75\pm0.05$ and $k=376\pm15$ h (fixed $A=100$). The insets show piezoresponse phase images acquired 3 h and 745 h after polarization reversal.

with the STO substrate (and also considering the potential PTO/STO interfacial energies) results in the situation that the tetragonal ferroelectric PTO film at 570 °C is thermodynamically more favorable (i.e., at low growth rate and proper substrate treatment) than the cubic paraelectric PTO film.[7] Although this increase in T_c under epitaxial strain is well known, since it results directly from including the mismatch strain in a Landau-Ginzburg-Devonshire (LGD) free energy,[7] the physical reasons for this behavior are not generally appreciated. The mismatch between the cubic PTO and the STO is large at the growth temperature, and the development of a coherent interface would cost excessive strain energy. Alternatively, relaxing the very thin initial cubic PTO film in order to form a semicoherent interface would cost excessive interfacial energy (see below). The energetically more favorable option for the system is to use the spontaneous strains present in the ferroelectric phase making the bulk unstable tetragonal PTO stable under this thin-film boundary condition.

Tetragonal ferroelectric single-domain PTO films will also occur at room temperature, because (1) we grow directly tetragonal ferroelectric single-domain PTO films at 570 °C, (2) they do not cross any T_c, and (3) the thermal expansion of the *a*-lattice parameters of tetragonal PTO and cubic STO are sufficiently similar. This provides the first reason why we observe monodomain films up to as large thickness as 340 nm as long as the growth rate is sufficiently low. However, it is not a sufficient reason. Another important reason is required, namely, that the critical thickness for the introduction of misfit dislocations is larger than 340 nm; this will be elaborated in Sec. IV B.

A. LGD model calculations

The completely *c*-oriented domain structure we observe is in agreement with the domain-stability maps of Pertsev *et al.*[7] and Alpay and Roytburd.[8] Our qualitative explanation can be quantified using the model of Pertsev *et al.* For the strain exerted by STO on the *cubic* PTO, where we use our measured lattice parameters (Fig. 5), Pertsev's model predicts a T_c increase from 492 °C to about 840 °C. Results of the model, i.e., the *a*-lattice and *c*-lattice parameter of PTO as a function of temperature, are presented in Fig. 5 as solid lines. It is important to note that not a single adjustable parameter was present in the model for calculating the solid lines. In this context the agreement with the *c*-axis value measured for the 130-nm-thick PTO film is exceptionally good.[29] The solid lines in Fig. 5 were calculated as follows.

The Gibbs-free energy *G* of a tetragonal ferroelectric thin film, elastically clamped to a cubic (001) substrate, with its *c* axis and polarization perpendicular to the substrate surface can be written in the framework of the LGD formalism as[7]

$$G = a_3^* P_3^2 + a_{33}^* P_3^4 + a_{111} P_3^6 + \frac{u_m^2}{s_{11}+s_{12}},$$

$$a_3^* = a_1 - u_m \frac{2Q_{12}}{s_{11}+s_{12}}, \quad a_{33}^* = a_{11} + \frac{Q_{12}^2}{s_{11}+s_{12}}, \qquad (1)$$

where a_1, a_{11}, and a_{111} are the dielectric stiffness coefficients at constant stress, s_{ij} are the elastic compliance coefficients at constant polarization, Q_{12} is a cubic electrostrictive coeffi-

cient in polarization notation, and u_m is the clamping or misfit strain in the film defined as $u_m=(b-a_0)/b$, with b and a_0 as the lattice parameters of the substrate and cubic unit cell of the free (unstrained) film, respectively. A minimum in Gibbs-free energy leads to a spontaneous polarization P_3 given by

$$P_3^2 = \frac{-a_{33}^* + [(a_{33}^*)^2 - 3a_3^* a_{111}]^{1/2}}{3a_{111}}, \tag{2}$$

and the spontaneous elastic strains x_i are given by $x_1=x_2=Q_{12}P_3^2$ and $x_3=Q_{11}P_3^2$. In the calculations for PTO all the parameters provided by Pertsev *et al.*[7] were used, which were in fact almost all based on the parameters provided by Haun *et al.*[26] Then it is assumed that Q_{11} and Q_{12} are constants independent of temperature. Also s_{ij} are assumed temperature independent, but a realistic 10% variation over the considered temperature range turned out not to affect significantly the results. In fact, the temperature dependence in the final results originates predominantly from a_1 [$=3.8(T-479)10^5$ with T in degree Celsius (Ref. 26)] and to lesser extent from u_m by considering the temperature-dependent lattice constants (see Fig. 5).

In between room temperature and 800 °C the STO lattice parameter was measured by us (using linear regression, see the fit to the STO data in Fig. 5) yielding

$$b(\text{Å}) = 3.905 + 3.61 \times 10^{-5} T(^\circ\text{C}). \tag{3}$$

At high temperatures (550–800 °C) we have direct experimental data for the lattice parameter of cubic PTO (see Fig. 5). We assume that the cubic PTO is fully relaxed although this is not the case (also see for discussion Ref. 29). At room temperature we do not have experimental access to the lattice parameter of strain-free cubic PTO. However, the a-lattice and c-lattice parameters of strain-free bulk ferroelectric PTO are well known at room temperature,[23] and the Q_{11} and Q_{12} values are known as well.[7,26] Then it is straightforward to calculate the a_0 of nonstrained cubic PTO at room temperature, 3.956 Å. Now, knowing a_0 both at room temperature and at high temperatures yields the following equation for strain-free cubic PTO as a function of temperature:

$$a_0(\text{Å}) = 3.955 + 4.73 \times 10^{-5} T(^\circ\text{C}), \tag{4}$$

which is presented as a dashed line in Fig. 5. The solid lines in Fig. 5 can now be calculated without any adjustable parameter left. In principle the result of Pertsev's model holds for any film thickness (of course above a minimum thickness related to the ferroelectric correlation length) because it only compares coherently matching single-domain PTO on STO. Therefore, the model predicts the same behavior for the 130- and 280-nm-thick PTO films. However, the experimental results show clear differences, particularly at high temperatures (>600 °C).

Indeed, upon heating to and cooling from 700 °C the 130-nm-film exhibits nearly identical behavior indicating that relaxation in this film does not occur appreciably even at a temperature as high as 700 °C. The film remains in a stable strained state. On the other hand, the results of the 280-nm film clearly indicate that relaxations start just above 600 °C and that the tetragonal ferroelectric state relaxes, probably by introduction of misfit dislocations, to the cubic paraelectric phase. As a matter of course this relaxation leads to a much faster transition from the strained ferroelectric tetragonal phase to the cubic phase than on the basis of Pertsev's model in which strain relaxation is not included. If it is assumed that the initial strain was 80% relaxed in the 280-nm film, the reappearance of the tetragonal ferroelectric phase upon cooling from 800 °C can be modeled excellently as it is indicated by the dashed-dotted line in Fig. 5. Then the T_c shifts back from about 840 °C–540 °C, which is still 50 °C higher than the T_c of bulk PTO. Also the development of the c lattice parameter below 540 °C is excellently reproduced, taking the amount of relaxation (80%) as the only adjustable parameter in Pertsev's model.

The explanation for the difference between the 130- and 280-nm-thick films is interesting. The total amount of strain energy stored in the thicker film is higher than in the thinner film. An energy barrier has to be overcome in order to nucleate dislocations and allow relaxation of the strain by misfit dislocations.[16,18,19] Heating provides the thermal energy to overcome this energy barrier. Therefore, the thicker the coherently matching film, the larger is the amount of stored strain energy in the film and the lower is the temperature where relaxation can start to occur. In other words, the critical film thickness for the introduction of misfit dislocations reduces considerably at these high temperatures,[16,18,19] and at 700 °C it is apparently still above 130 nm but below 280 nm.

The present results are in agreement with the experimental observation obtained by Janolin *et al.*[22] and provides further proof for their conclusion that the film already adopts a tetragonal symmetry during deposition at a temperature clearly higher than the T_c of bulk PTO. Their temperature-dependent XRD results show that a 100-nm PTO film grown at a temperature of 577 °C is in a tetragonal ferroelectric state. The measured values for the a-lattice and c-lattice parameters of the PTO film at the growth temperature disagree with a coherently elastically strained cubic phase, just distorted via Poisson's ratio to become a tetragonal phase, because this would result in a much smaller c-lattice parameter than observed. The actual c-lattice parameter measured by us and Janolin *et al.* indicate that the spontaneous strains of the tetragonal ferroelectric phase have come into play to achieve a proper coherent matching at the deposition temperature without requiring large internal stresses within the PTO; in this sense the calculated deposition stress of −1.8 GPa (Ref. 22) should only be considered as hypothetical.

B. Comparison between the Matthews-Blakeslee and the People-Bean models

A crucial point to address is the calculation of the critical film thickness signaling the onset of relaxation by misfit dislocations. As explained in the introduction the MB model predicts too low values for the critical thickness of ferroelectric films, particularly in case of high quality substrate-film interfaces and low strains. Alternative models were developed, explaining better the observed critical thickness in

semiconductor thin films[16,17] or explaining both metals and semiconductors.[18,19] A drawback of the latter type of model is that it requires additional unknown parameters. To keep the situation tractable, we will perform simple calculations not requiring unknown parameters and compare the critical thickness h_c according to the models of MB and of People and Bean (PB).[16] The PB model is phenomenological because it explains experimental data for semiconductor films clearly better than the MB model, but its theoretical drawbacks have also been outlined.[30] For the MB model we used the equation given by Speck and Pompe,[6] and for the PB model the equation given by Marée *et al.*;[17]

$$h_c^{\mathrm{MB}} = \frac{\bar{b}(1-\nu\cos^2\beta)}{8\pi\cos\lambda(1+\nu)}\frac{1}{\varepsilon}\ln\left(\alpha\frac{h_c}{\bar{b}}\right), \tag{5a}$$

$$h_c^{\mathrm{PB}} = \frac{\bar{b}(1-\nu)}{40\pi(1+\nu)}\frac{1}{\varepsilon^2}\ln\left(\frac{h_c}{\bar{b}}\right), \tag{5b}$$

where $\bar{b}$ is the magnitude of the Burgers vector, ν is the Poisson's ratio, ε is the misfit strain, α is the cut-off parameter used to describe the continuum energy of the dislocation core, β is the angle between the dislocation line and the Burgers vector, and λ is the angle between the Burgers vector and line that lies within the interface and in a plane normal to the dislocation line. We assume misfit dislocations in PTO with Burgers vector of type $\langle 110\rangle$ (α=4, β=90°, and λ=45°)[6] and a Poisson's ratio of 0.33. In both cases two strains holding at the deposition temperature (570 °C) will be the input for the calculations. The strain based on the difference between the lattice parameter of the STO substrate, b, and the cubic paraelectric film, a_0, or between b-lattice and a-lattice parameters of the tetragonal ferroelectric film. Lattice parameters can be directly extracted from the experimental or theoretical data also shown in Fig. 5 and Eqs. (3) and (4). For cubic PTO on STO the critical thickness according to the MB and PB models is 6.2 (Ref. 31) and 48 nm, respectively. However, for the tetragonal PTO on STO the critical thickness according to the MB and PB models is 19 and 386 nm, respectively. Comparing these results with our observations makes clear that the MB model gives too low critical thickness values and that our observation that a 340-nm-thick tetragonal (completely c oriented) PTO film is still coherent with the STO is in agreement with a model that predicts a critical thickness beyond this value for a film that is directly grown in the tetragonal phase. Even when relaxation by misfit dislocations occurs, it can be a partial relaxation, still maintaining sufficient strain to stabilize during growth the tetragonal ferroelectric phase at temperatures clearly higher than bulk T_c. This situation applies to $Pb(Zr_xTi_{1-x})O_3$ films on (001)-STO (Refs. 32 and 33) at relatively small thickness and probably will occur for PTO films at larger thickness than the ones we have grown in the present work.

V. CONCLUSIONS

Fully c-axis oriented PTO films on STO substrates were grown up to 340 nm thickness after optimizing growth conditions. PFM measurements prove ferroelectric behavior with sufficiently long retention times in our films. The influence of the deposition rate and substrate-surface treatment on the growth condition has been established. The experiments prove that relatively thick (at least 280 nm) coherent monodomain PTO films on (001)-STO can be achieved using low growth rates (laser-pulse frequency $\leq$5 Hz). When increasing the growth rate (5–15 Hz frequency) a domains develop above a critical thickness whose value is rapidly decreasing from above 250 nm to below 70 nm.

Although deposited at a temperature well above the T_c of bulk PTO, our films grow directly in a coherently matched ferroelectric state. Due to the coherency strains the T_c of the films is at least 200 °C higher than of bulk PTO. The thickness of the coherent films is much larger than the critical thickness for strain relaxation predicted by the Matthews-Blakeslee model and suggests better agreement with the People and Bean model. The temperature evolution of the a-lattice and c-lattice parameter of the ferroelectric films agrees well with the model of Pertsev *et al.*[7] The present work clarifies that the 20% of a domains predicted by the model of Koukhar *et al.*[9] for PTO on (001)-STO, which is supported by data points and widely adopted in literature[2,3] for PTO films thicker than 10 nm, is not necessarily the equilibrium solution. This solution is applicable if the initial PTO film is relaxed during growth by misfit dislocations into the cubic paraelectric phase. This relaxation is facilitated if the substrate or film quality is not optimal (e.g., dislocations are already present). Instead, for the present work the monodomain model of Pertsev *et al.*[7] applies but for a much larger film thickness than considered feasible up to now.

ACKNOWLEDGMENTS

This work was funded by the Zernike Institute for Advanced Materials, University of Groningen, The Netherlands. A.V. and B.N. gratefully acknowledge the Dutch/National Science Foundation (NWO/VIDI) for financial support.

*Corresponding author; b.j.kooi@rug.nl

[1] M. Dawber, K. M. Rabe, and J. F. Scott, Rev. Mod. Phys. **77**, 1083 (2005).

[2] D. G. Schlom, L. Q. Chen, C. B. Eom, K. M. Rabe, S. K. Streiffer, and J. M. Triscone, Annu. Rev. Mater. Res. **37**, 589 (2007).

[3] N. Setter, D. Damjanovic, L. Eng, G. Fox, S. Gevorgian, S. Hong, A. Kingon, H. Kohlstedt, N. Y. Park, G. B. Stephenson, I. Stolitchnov, A. K. Tagantsev, D. V. Taylor, T. Yamada, and S. Streiffer, J. Appl. Phys. **100**, 051606 (2006).

[4] J. H. Haeni, P. Irvin, W. Chang, R. Uecker, P. Reiche, Y. L. Li, S. Choudhury, W. Tian, M. E. Hawley, B. Craigo, A. K. Tagantsev,

S. Q. Pan, S. K. Streiffer, L. Q. Chen, S. W. Kirchoefer, J. Levy, and D. G. Schlom, Nature (London) **430**, 758 (2004).
[5] K. J. Choi, M. Biegalski, Y. L. Li, A. Sharan, J. Schubert, R. Uecker, P. Reiche, Y. B. Chen, X. Q. Pan, V. Gopalan, L.-Q. Chen, D. G. Schlom, and C. B. Eom, Science **306**, 1005 (2004).
[6] S. Speck and W. Pompe, J. Appl. Phys. **76**, 466 (1994).
[7] N. A. Pertsev, A. G. Zembilgotov, and A. K. Tagantsev, Phys. Rev. Lett. **80**, 1988 (1998).
[8] P. Alpay and A. L. Roytburd, J. Appl. Phys. **83**, 4714 (1998).
[9] V. G. Koukhar, N. A. Pertsev, and R. Waser, Phys. Rev. B **64**, 214103 (2001).
[10] Y. L. Li, S. Y. Hu, Z. K. Liu, and L. Q. Chen, Acta Mater. **50**, 395 (2002).
[11] A. G. Zembilgotov, H. Kohlstedt, N. A. Pertsev, and R. Waser, J. Appl. Phys. **91**, 2247 (2002).
[12] S. K. Streiffer, J. A. Eastman, D. D. Fong, Carol Thompson, A. Munkholm, M. V. Ramana Murty, O. Auciello, G. R. Bai, and G. B. Stephenson, Phys. Rev. Lett. **89**, 067601 (2002).
[13] D. D. Fong, G. B. Stephenson, S. K. Streiffer, J. A. Eastman, O. Auciello, P. H. Fuoss, and C. Thompson, Science **304**, 1650 (2004).
[14] Q. Y. Qiu, V. Nagarajan, and S. P. Alpay, Phys. Rev. B **78**, 064117 (2008).
[15] J. W. Matthews and A. E. Blakeslee, J. Cryst. Growth **27**, 118 (1974).
[16] R. People and J. C. Bean, Appl. Phys. Lett. **47**, 322 (1985); **49**, 229 (1986).
[17] P. M. J. Marée, J. C. Barbour, J. F. van der Veen, K. L. Kavanagh, C. W. T. Bulle-Lieuwma, and M. P. A. Viegers, J. Appl. Phys. **62**, 4413 (1987).
[18] B. A. Fox and W. A. Jesser, J. Appl. Phys. **68**, 2801 (1990).
[19] G. L. Price, Phys. Rev. Lett. **66**, 469 (1991).
[20] Z. Li, C. M. Foster, D. Guo, H. Zhang, G. R. Bai, P. M. Baldo, and L. E. Rehn, Appl. Phys. Lett. **65**, 1106 (1994).
[21] I. Vrejoiu, G. Le Rhun, L. Pintilie, D. Hesse, M. Alexe, and U. Gösele, Adv. Mater. **18**, 1657 (2006).
[22] P. E. Janolin, F. Le Marrec, J. Chevreul, and B. Dkhil, Appl. Phys. Lett. **90**, 192910 (2007).
[23] S. A. Mabud and A. M. Glazer, J. Appl. Crystallogr. **12**, 49 (1979).
[24] G. Koster, B. Kropman, G. Rijnders, D. H. A. Blank, and H. Rogalla, Appl. Phys. Lett. **73**, 2920 (1998).
[25] G. Rispens and B. Noheda (private communication).
[26] M. J. Haun, E. Furman, S. J. Jang, H. A. McKinstry, and L. E. Cross, J. Appl. Phys. **62**, 3331 (1987).
[27] A. Gruverman, H. Tokumoto, A. S. Prakash, S. Aggarwal, B. Yang, M. Wuttig, R. Ramesh, O. Auciello, and T. Venkatesan, Appl. Phys. Lett. **71**, 3492 (1997).
[28] W. S. Ahn, W. W. Jung, S. K. Choi, and Y. Cho, Appl. Phys. Lett. **88**, 082902 (2006).
[29] The excellent agreement is partly related to the following two factors that largely cancel each other: Firstly, we use a too high cubic PTO lattice parameter (a_0) at high temperatures, because the data originates from a partially strained film. Using a lower a_0 value will also lower the calculated c values at higher temperatures. Secondly, we neglect the additional increase in c-lattice parameter due to Poisson's effect when at these higher temperatures, by compressive stresses, the a-lattice parameter of the tetragonal ferroelectric is coherently matched with the STO lattice parameter.
[30] S. M. Hu, J. Appl. Phys. **69**, 7901 (1991).
[31] The 6.2-nm critical thickness calculated is substantially lower than the 14 nm calculated in Ref. 6 for identical conditions. The reason is that a higher strain value has been used compared to Ref. 6, but our strain value is consistent with the STO lattice parameter and cubic paraelectric PTO lattice parameter we measured using temperature-dependent XRD (cf. Fig. 5).
[32] S. Gariglio, N. Stucki, J.-M. Triscone, and G. Triscone, Appl. Phys. Lett. **90**, 202905 (2007).
[33] P. E. Janolin, B. Fraisse, F. Le Marrec, and B. Dkhil, Appl. Phys. Lett. **90**, 212904 (2007).